

Lasers in Manufacturing Conference 2019

Correlation between Joint Strength and Process Temperature in Quasi-Simultaneous Laser Transmission Welding of Polyamide 6

Anton Schmailzl^{a,*}, Benjamin Quandt^a, Stefan Hierl^a, Michael Schmidt^{b,c,d}

^a*Ostbayerische Technische Hochschule Regensburg, Galgenbergstraße 30, 93053 Regensburg, Germany*

^b*Bayerisches Laserzentrum GmbH, Konrad-Zuse-Straße 2-6, 91052 Erlangen, Germany*

^c*Erlangen Graduate School in Advanced Optical Technologies, Paul-Gordan-Straße 6, 91052 Erlangen, Germany*

^d*Chair of Photonic Technologies, Friedrich-Alexander-Universität Erlangen-Nürnberg, Paul-Gordan-Straße 3, 91052 Erlangen, Germany*

Abstract

The joint strength is gaining importance in quasi-simultaneous laser transmission welds, especially in structural components. A correlation between the joint strength and a process characteristic is a basic requirement for selecting the best process parameter setting. In this work, the temperature is measured during welding polyamide 6 by using a scanner-integrated pyrometer with an InGaAs-detector. The filtering of the heat radiation in the upper joining partner is taken into account by calibrating the measurement system. By this, the measured temperature signal represents the temperature in the joining zone. A correlation is found between the measured temperature and the resulting joint strength. Moreover, high joint strengths are also seen for welds with short welding times, as far as the temperature is sufficiently high. With this knowledge, a process window can be derived easily in order to produce welds with high strength and short welding times.

Keywords: laser transmission welding, pyrometer, temperature, joint strength, welding time;

1. Introduction

The quasi-simultaneous laser transmission welding is typically used in the automotive and the medical industry. The precise heating without generating particles is the key advantage (Klein, 2012). The process is gaining more and more importance in the production of structural parts (Jaeschke et. al, 2015). The

* Corresponding author. Tel.: +49 941 943 9876

E-mail address: anton2.schmailzl@oth-regensburg.de

temperature in the weld seam is a promising process characteristic for process design. The main challenge is to measure the temperature in the core of the weld seam (Lakemeyer, 2018). On one hand the detection spot should be small sized, on the other hand the attenuation of the heat radiation by the optics should be low, as found in a previous study (see Schmailzl et. al, 2018).

In this article, the temperature is measured with a scanner-integrated pyrometer as well as with a stationary mounted one. Both pyrometers are characterized and calibrated for the measurement task. The set-path progression and the process times are measured, additionally. The measured signals are used to characterize the process. Finally, these process characteristics are compared with the joint strength of welded samples.

2. Experimental setup

Figure 1 shows a scheme of the experimental setup, which is used for the welding experiments. The system, especially the optical path of the 3D-scanner with the integrated pyrometer is described in Schmailzl et. al, 2018.

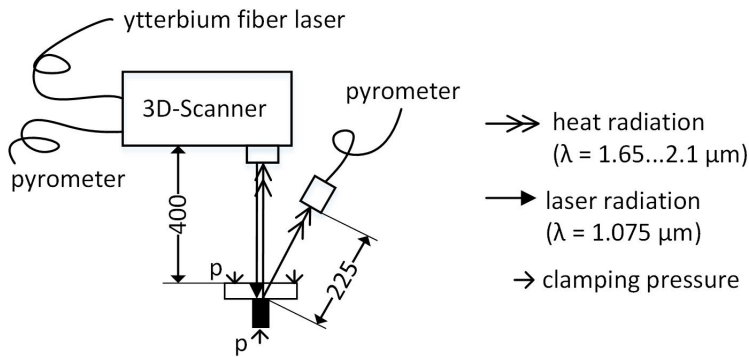


Fig. 1. Scheme of the experimental setup: 3D-scanner with integrated pyrometer, stationary mounted pyrometer, clamping device.

The coaxial arrangement between the laser beam and the optical path of the heat radiation is analyzed by measuring the centroids of two guide-lasers, which are integrated in each optical path. Therefore, a CMOS-camera is used. The coaxial error is found to be 0.25 ± 0.05 mm.

The pyrometer is calibrated, since the received heat radiation is attenuated by the scanner optics. For this task, the temperature is measured on a black body emitter, which is placed at the position of the clamping device. The temperature of the black body emitter is varied. The dependency between the black body temperature and the measured temperature is used as a calibration curve. By this, the temperature signal is adjusted in a post-processing, using the calibration curve. Finally, the temperature signal is equal to the black body emitter. The heat radiation during welding mainly comes from the joining area. Thus, the upper polymer also attenuates the heat radiation. In order to take this also into account, a polyamide sample with a thickness of $t = 2$ mm is placed above the black body radiator. In the calibration it is found, that the pyrometer is sensitive for a black body temperature between $T = 207...527$ °C.

A second pyrometer is used additionally. Here, the heat radiation is not additionally attenuated by scanner optics, which allows the measuring of lower temperatures. This pyrometer is stationary mounted and focused to the mid position of the joining trajectory. By using the above-mentioned calibration procedure, the threshold temperature is found to be $T = 107$ °C. Both pyrometers are sensitive in the range

of $\lambda = 1.65 \dots 2.1 \text{ } \mu\text{m}$ and have a sampling frequency of $f = 50 \text{ kHz}$. The scanner-integrated pyrometer has a detection spot diameter of $\varnothing 1.7 \text{ mm}$, whereas the second one has a diameter of $\varnothing 2.9 \text{ mm}$.

3. Experimental procedure

Injection molded polyamide 6 plates (Ultrad B3s) with a thickness of $t = 2 \text{ mm}$ are arranged in a T-joint configuration. The lower polymer has a carbon black content of 1 wt.-%. The contact surface of the lower polymer is milled, in order to ensure a good contact situation. The samples are welded, using a laser beam diameter of $\varnothing 4.5 \text{ mm}$. Figure 2 shows the position of the T-joint relative to the scanner (a) as well as the scanning procedure (b):

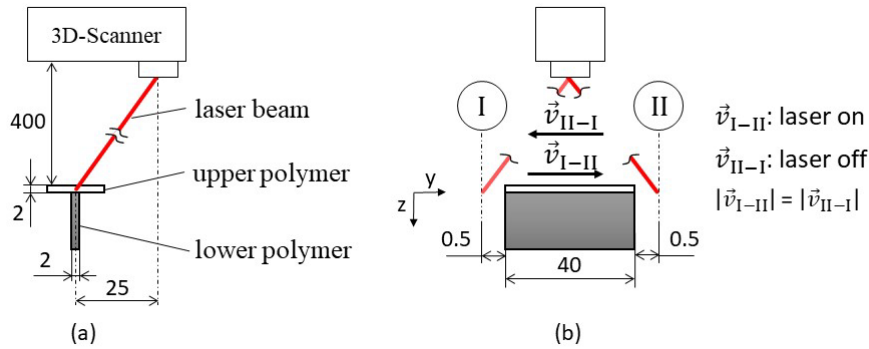


Fig. 2. (a) Position of the scanner and the polymer samples; (b) scanning procedure

The laser beam is deflected with a feed rate of $v = 2100 \text{ mm/s}$ from position I to position II with laser on. Afterwards, the laser is turned off and the laser beam is moved back to position I (see figure 2 (b)). This scanning procedure is repeated until the set-path criterion of $s_c = 0.5 \text{ mm}$ is reached. The samples are clamped for further three seconds after the set-path criterion is reached. This time sequence is referred as post-irradiation time (t_N).

Nine process parameter sets are performed by variation of the laser power and the joining pressure in the joining area (see table 1). Seven welds are performed for each process parameter setting. The plastic samples are dried for 10 h at $T = 80 \text{ } ^\circ\text{C}$ before welding.

Table 1. Process parameter settings (I-IX) for the welding experiments.

	I	II	III	IV	V	VI	VII	IIIX	IX
joining pressure p_f [MPa]	3.0	1.0	0.5	3.0	1.0	0.5	3.0	1.0	0.5
laser power P [W]	50	50	50	125	125	125	200	200	200

After welding, the tensile strength is evaluated at a testing speed of 50 mm/s . Before testing, the samples are conditioned to 2.5 % water content, which is the saturation value at room temperature ($T = 23 \text{ } ^\circ\text{C}$) and a relative humidity of 50 % water in air. The short time weld factor ζ_k is calculated according to DVS 2203, in order to compare the resulting joint strength with the strength of the base material.

$$\zeta_k = \frac{\sigma_w}{\sigma_r} \quad (1)$$

The joint strength σ_w is the force at break divided by the cross-section of the weld seam (80 mm²). An enlargement of the load bearing area by the squeezed-out material is not taken into account. The strength of the base material (σ_r) is tested by using a specimen geometry according to ISO 527.

4. Evaluation of the detected heat radiation

The pyrometers are receiving heat radiation, emitted from both joining partners. Therefore, the received heat radiation in the spectral sensitivity range of the pyrometer is calculated on basis of a computed temperature field, in order to determine the proportion of heat radiation emitted from each joining partner. Figure 3 shows the temperature field at $t = 1.2$ s, computed in a thermo-mechanical finite element simulation. The process parameter setting V is used.

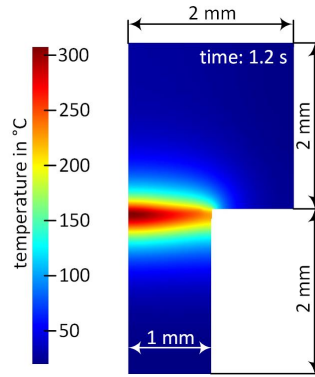


Fig. 3. Computed temperature field for the process parameter setting V, using a thermo-mechanical process simulation.

The temperature in the optical axis is used for the calculation of the detected heat radiation. The lower polymer is approximated as a black body emitter by using an emissivity coefficient of $\varepsilon = 1$. The spectral attenuation of the heat radiation in the upper polymer is taken into account as well. The detected heat radiation, emitted from the semi-transparent upper polymer is calculated according to DeWitt, 1988. Hereby, the upper polymer is divided into layers with a thickness of five microns. The emission of a single layer is calculated on basis of the corresponding temperature in the optical axis. The spectral emissivity as well as the attenuation of the heat radiation due to absorption is also taken into account.

The received heat radiation, emitted from the upper polymer is found by summing the emission of each layer. Then, the emission of the lower and the upper polymer is compared. It is found, that 98 % of the total heat radiation is emitted from the lower polymer. The spectral range of the pyrometer leads to an exponential dependency between the received heat radiation and the displayed temperature. By this, the significant higher temperatures in the joining area are stronger weighted than those in the upper polymer. In addition, the emissivity is much higher in the lower polymer. Thus, the heat radiation from the upper polymer is negligible small. Hence, the measured temperature can be interpreted as the core temperature of the weld seam, by taking only the filtering of the heat radiation in the upper polymer into account.

5. Process characteristics

The temperature (T), the process time (t), the current position of the laser beam (y) as well as the set-path (s) is measured, using a real time control system. Figure 4 (a) shows the temperature course of the scanner-integrated pyrometer (T_{P1}) and the one of the stationary mounted pyrometer (T_{P2}) as well as the set-path progression (s) against time (t) for the process parameter setting V.

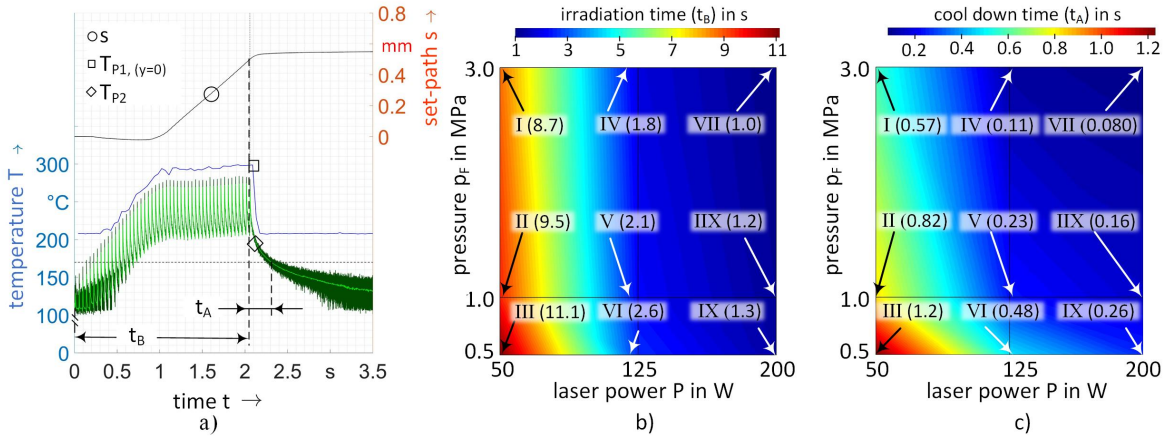


Fig. 4. (a) Course of the temperature in the mid position of the weld trajectory ($y = 0$), measured with both pyrometers (T_{P1} , T_{P2}) as well as the set-path progression (s) of a weld with parameter setting V; (b) irradiation time t_B ; (c) cool down time t_A

A single scan is clearly seen in the course of T_{P2} . The temperature course T_{P1} is an excerpt of the temperature signal, by using the scanning procedure in fig. 2 (b). The data points of T_{P1} are in the mid-position of the weld trajectory ($y = 0$) and with laser on. The starting point of the temperature plateau correlates with the beginning of the stationary process state, as seen by comparing the temperature courses with the set-path progression (see fig. 4 a). The temperature of the scanner-integrated pyrometer is just slightly higher than the temperature of the second pyrometer. The temperature decreases rapidly, after the set-path criterion is reached, since the laser is switched off. As the temperature is decreasing, the signal T_{P2} is becoming noisier.

The irradiation time (t_B) reduces by an increase in laser power and joining pressure (see fig. 4, b). The time span until the temperature signal T_{P2} is reduced to $T = 170\text{ }^{\circ}\text{C}$ is referred as cool down time (t_A). The cool down time also reduces by increasing laser power and joining pressure (see fig. 4, c). The cool down time is a characteristic value for the recrystallization time. The recrystallization temperature is found to be $T = 185\text{ }^{\circ}\text{C}$ in a DSC-analysis.

6. Correlation between joint strength and quasi-stationary process temperature

Figure 5 (a) shows the arithmetic mean of the weld factor for each process parameter setting in a bar diagram, as well as the corresponding mean of the quasi-stationary temperature (T_{P2}). The cross sections of representative welds are shown in figure 5 (b).

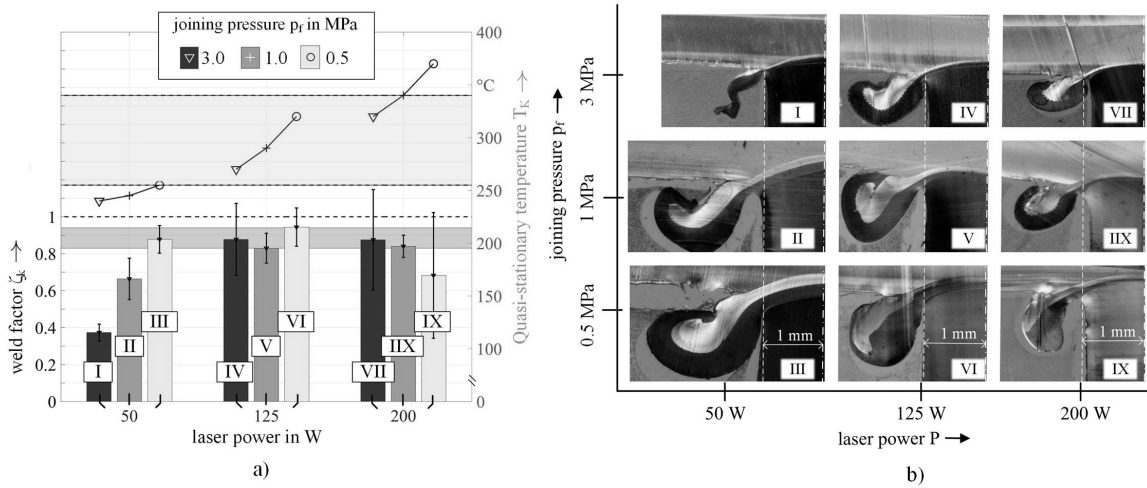


Fig. 5. (a) Weld factor and quasi-stationary temperature for the process parameter settings I-IX; (b) half of the cross-section of representative welds.

The quasi-stationary temperature is increasing with decreasing joining pressure and increasing laser power. Hence, it is increasing with ascending number of the roman numeral. A weld factor between $\zeta_k = 0.83 \dots 0.94$ is reached for the settings III-IX (see shaded area in bar plot). Here, the joint strength of the weld is very close to the one of the base material ($\sigma_r = 48.2 \text{ MPa} \pm 1.2 \text{ MPa}$). A significant reduced weld factor is seen for the remaining rest of the process settings (see I, II, IX).

Some error bars are exceeding the weld factor $\zeta_k = 1$. However, this does not mean that the strength of the joint is higher than the strength of the base material. The squeezed-out material is slightly enlarging the load-bearing area, as can be seen on the thin-cuts in fig. 5 (b). In general, the consideration of this effect would lead to reduced weld factors. However, the impact of the enlarging area on the weld factor is not taken into account, since the load bearing area cannot be measured precisely enough.

No significant correlation between weld factor and quasi-stationary temperature is found regarding the sets III-IX. In contrast, a clear correlation between the quasi-stationary temperature and the weld factor is given for the settings I-III. It is to state, that the joint strength decreases with increasing joining pressure, since the quasi-stationary temperature is decreased. The temperature of set III ($T = 251^\circ\text{C}$) can be interpreted as a threshold value. Above this temperature, a saturation limit for the joint strength is reached for the herein shown parameter settings.

Some welds in IX are showing craters with a smooth surface in the fractured area of the weld seam. This indicates the presence of bubbles in the weld seam and signalizes thermal damage of the material. These welds have a low weld factor of approximately $\zeta_k \approx 0.2$. In contrast, the welds without bubbles have a very high weld factor, comparable to those in IIX. As a result, an arithmetic mean value of $\zeta_k = 0.68$ and a comparatively high standard deviation is given for welds with setting IX.

In summary, the quasi-stationary temperature is too low at I and II and too high at IX, which leads to reduced joint strengths. For the herein shown experiments, a process window is to evaluate on basis of the given temperature range $T = 251 \dots 330^\circ\text{C}$. The recommended temperature for the hot plate ($T = 290^\circ\text{C}$) in hot plate welding (see Brüssel, 1999) and the one recommended for the mass temperature in injection molding ($T = 260^\circ\text{C}$) are included in the aforementioned temperature range.

The process parameter setting VII leads to a high joint strength as well as to the shortest irradiation time. Here, the irradiation time is just $t_B = 1.0$ s and the cool down time is just $t_A = 0.080$ s. This shows, that the joint strength is also high for very short irradiation times. Moreover, the short cool down time signalizes, that the post-irradiation time (t_N) can be also very short.

The melt layer thicknesses in both joining partners are decreasing with an increase in laser power and joining pressure (see fig. 5, b). A correlation between weld factor and a melt layer thickness of one joining partner is not to extract. To note is, that the melt layer thickness in the upper polymer is just a few hundredth of a millimeter for the setting IX (≈ 0.04 mm) and nearly five times lower than the one for the setting I (≈ 0.2 mm). Thus, the melt layer thickness is found to be no direct indicator for the joint strength.

7. Summary and outlook

In this work, the core temperature during quasi-simultaneous laser transmission welding of polyamide 6 T-joints is measured. The laser power and the joining pressure are varied. The joint strength of the welds are close to the one of the base material. A direct correlation between the quasi-stationary temperature and the joint strength is found. A temperature range is extracted, which leads to welds with a high joint strength. Within this range, no correlation is found between the quasi-stationary temperature and the joint strength. The joint strength reaches a saturation limit as far as the lower temperature threshold of the temperature range is reached. The exceeding of the upper temperature threshold leads to thermal damage of the material. The temperature range can be interpreted as a process window. However, the melt layer thicknesses in both joining partners and the irradiation time are found to be no direct indicator for the resulting joint strength. Moreover, the joint strength is also very high for welds with very short irradiation time and short time for cooling. This knowledge enables the improvement of the process design, in order to produce welds with high strength and low welding times.

Acknowledgements

The authors want to thank the Bavarian State Ministry of Economy and Media, Energy and Technology for funding the project THECOS in the Czech-Bavarian Cross-Border Cooperation Program INTERREG V-A.

References

- Brüßel, A., 1999. Fertigungstechnische und werkstoffspezifische Aspekte zum Fügen von Thermoplasten mittels Heizelement. Dissertation, Paderborn.
- DeWitt D. P., Nutter G. D., Theory and Practice of Radiation Thermometry. New York: Wiley, 1988.
- Jaeschke, P., Wippo, V., Suttman, O., Overmeyer, L., 2015. Advanced laser welding of high-performance thermoplastic composites. Journal of Laser Applications 27, S29004. 10.2351/1.4906379.
- Klein, R., 2012. Laser welding of plastics. Wiley-VCH, Weinheim, viii, 251.
- Lakemeyer, P., 2018. Entwicklung und Analyse neuartiger Verfahrensvarianten zum quasisimultanen Laserdurchstrahlschweißen unter Berücksichtigung der Temperaturentwicklung. Dissertation, Shaker Verlag, Aachen.
- Schmailzl, A., Quandt, B., Schmidt, M., Hierl, S., 2018. In-Situ process monitoring during laser transmission welding of PA6-GF30. Procedia CIRP 74, 524–527. 10.1016/j.procir.2018.08.131.